

Synchronization of two bacterial flagella as a stochastic process

Jing Qin and Nariya Uchida*

Department of Physics, Tohoku University, Sendai 980-8578, Japan

(Dated: March 28, 2025)

Synchronization with noise is important for understanding biophysical processes at nano- and micro-meter scales, such as neuronal firing and flagellar rotations. To understand the energetics of these processes, stochastic thermodynamics approaches are useful. Due to large fluctuations in a small system, ensemble averages of thermodynamic quantities are not sufficient to characterize the energetics of an individual sample. In this paper, we use a model for synchronization of bacterial flagella as an example, and develop an approximation method for analyzing the phase and heat dissipation in trajectories for different noise realizations. We describe the temporal evolution of the phase difference and heat dissipation as stochastic processes, and verify the analytical results by numerical simulations.

I. INTRODUCTION

Synchronization is ubiquitously seen in Nature. Since Huygens' discovery of synchronization in two pendulum clocks, the study of synchronization has expanded across various fields [1, 2]. In biological systems, synchronization plays a critical role in maintaining vital functions, such as regulating circadian rhythms [3], coordinating brain activity [4], and swimming using flagella and cilia [5–7].

Flagella and cilia provide a classical example of synchronization driven by hydrodynamic interactions, generating considerable interest in the field [8, 9]. Powered by molecular motors, these active filaments create rhythmic fluid movements that propel microorganisms forward. The power and recovery strokes of eukaryotic flagella and cilia are incorporated to reproduce metachronal waves through long-range hydrodynamic interactions [6, 7, 10–13], while other forms of interactions also contribute to coordinated beating [14–18]. Bacterial flagella have rotating helical bodies that are synchronized to form a bundle [19–21]. The cyclic motion of flagella and cilia are frequently represented by phase oscillators [9], and experimentally modeled by orbiting colloidal particles [22]. Additionally, as flagella operate at microscopic scales, thermal fluctuations and/or motor-induced active noises significantly influence their movement [23], sometimes causing order-disorder transitions [24]. Therefore, it is essential to consider stochastic effects alongside deterministic dynamics.

Numerous studies have examined synchronization under the influence of noise [1, 25–28]. For instance, in Ref. [27], the authors explored a generic model of two phase oscillators, showing that synchronization minimizes energy dissipation associated with the odd part of the coupling, while the even part has a contribution of either positive or negative sign depending on the specifics of the model. In Ref. [28], the authors discussed the energetics of cilia using the noisy Kuramoto model, and

showed that synchronization reduces dissipation. The energetics involved in synchronization are critical for understanding power efficiency in living systems [29]. However, many studies focus on noise-averaged quantities, which may overlook significant fluctuations for each sample. The rotation of individual bacterial flagella can be measured using the tethered cell method [30], in which the cell body is tethered to a glass substrate by the flagellum and rotates, or the bead assay [31, 32], where a spherical bead is attached to the flagellum and rotates. The latter method has the advantage of imposing a smaller load on the flagellum compared to the tethered cell method, and the hydrodynamic drag force on the bead is easier to estimate. The load can be further reduced by modifying the hook, allowing for precise measurement of large speed fluctuations [33].

In this paper, we examine a specific model of two bacterial flagella with cyclic trajectories influenced by white noise. This model allows us to analytically investigate not only the statistical properties but also the single-trajectory dynamics without averaging. We validate our theoretical findings through numerical simulations.

II. MODEL

Following Ref. [34], we consider flagella tethered to a substrate as active rotors that move by pumping the fluid. We take the xy -coordinates on the substrate and assume that a pair of rotors are fixed on it with distance d along the x -axis, as shown in Fig. 1. Each rotor has a spherical bead of radius a , which is connected to the substrate by an L-shaped filament. The filament consists of a vertical shaft of height h , which is the rotation axis of the rotor, and a horizontal arm with length b , which gives the radius of the circular trajectory of the bead. Using the polar angle ϕ_i of the i -th rotor, the positions of the two beads are represented by $\mathbf{r}_1 = h\mathbf{e}_z + b\mathbf{n}_1$ and $\mathbf{r}_2 = d\mathbf{e}_x + h\mathbf{e}_z + b\mathbf{n}_2$, where \mathbf{e}_i ($i = x, z$) is the unit vector along the x - and z -axis, respectively, and $\mathbf{n}_i(t) = (\cos\phi_i(t), \sin\phi_i(t), 0)$ gives the direction of the rotor's arm. The velocity of the bead reads $\mathbf{v}_i = \frac{d}{dt}\mathbf{r}_i = b\frac{d}{dt}\mathbf{n}_i = b\frac{d\phi_i}{dt}\mathbf{t}_i$, where $\mathbf{t}_i = (-\sin\phi_i, \cos\phi_i, 0)$

* uchida@cmpt.phys.tohoku.ac.jp

is the unit tangential vector of the orbit.

A tethered flagellum pumps the surrounding fluid by the activity of the flagellar motor, which is modeled by a constant force exerted by the bead on the fluid. We decompose the force \mathbf{F}_i exerted by the i -th bead ($i = 1, 2$) as $\mathbf{F}_i = F_r \mathbf{n}_i + F_\phi \mathbf{t}_i + F_z \mathbf{e}_z$, where F_r, F_ϕ, F_z are constants. In a low Reynolds number condition, the forces generate the flow velocity field $\mathbf{v}(\mathbf{r}) = \mathbf{G}(\mathbf{r} - \mathbf{r}_1) \cdot \mathbf{F}_1 + \mathbf{G}(\mathbf{r} - \mathbf{r}_2) \cdot \mathbf{F}_2$, where \mathbf{G} is the Green function of the Stokes equation. The Green function under the no-slip boundary condition on the substrate is known as the Blake tensor [35]. For $\mathbf{r} = \mathbf{r}_2 - \mathbf{r}_1 \simeq d \mathbf{e}_x$ with $d \gg h, b, a$, we obtain $\mathbf{G}(\mathbf{r}) \simeq 3h^2/(2\pi\eta d^3) \mathbf{e}_x \mathbf{e}_x$, where η is the shear viscosity.

In the overdamped limit, the motion of rotors is determined by the balance of three forces: the driving force, the resistance force and the thermal fluctuation force. The driving force is the reaction of the force exerted by the flagellum on the fluid and is given by $-F_\phi \mathbf{t}_i$ for the i -th rotor. The tangential component of the viscous resistance force is given by $F_{\text{viscous}} = \mathbf{t}_i \cdot \zeta (\frac{d}{dt} \mathbf{r}_i - \mathbf{v}(\mathbf{r}_i))$, where $\zeta = 6\pi\eta a$ is the resistance coefficient. The thermal fluctuation force is $F_{\text{thermal}} = \sqrt{2k_B T \zeta} \xi_i$, where ξ_i is a white Gaussian noise satisfying $\langle \xi_i(t) \xi_i(t') \rangle = \delta(t - t')$. It is defined as $\xi_i = dW_t^{(i)}/dt$ using the standard Wiener process $W_t^{(i)}$, and has the dimension of $t^{-\frac{1}{2}}$. The equation of force balance $-F_\phi + F_{\text{viscous}}^{(i)} + F_{\text{thermal}}^{(i)} = 0$ gives the Langevin equation,

$$\zeta b \frac{d\phi_1}{dt} = -F_\phi + \frac{9ah^2}{d^3} (F_\phi \sin \phi_2 - F_r \cos \phi_2) \sin \phi_1, \quad (1)$$

$$+ \sqrt{2k_B T \zeta} \xi_1$$

$$\zeta b \frac{d\phi_2}{dt} = -F_\phi + \frac{9ah^2}{d^3} (F_\phi \sin \phi_1 - F_r \cos \phi_1) \sin \phi_2 \quad (2)$$

$$+ \sqrt{2k_B T \zeta} \xi_2.$$

We assume $F_\phi < 0$ so that each rotor has a positive intrinsic phase velocity. Let $F = \sqrt{F_\phi^2 + F_r^2}$ and $\beta = \arctan(-F_\phi/F_r)$ ($0 \leq \beta \leq \pi/2$). As shown in Fig. 1, β represents the tilt of the force from the radial direction, which can be originated from the deviation of the flagellar axis from the anchoring point. For convenience, we introduce the two characteristic frequencies $\omega = F/(\zeta b)$ and $\omega_\phi = -F_\phi/(\zeta b)$ with the relation $\omega_\phi = \omega \sin \beta$. We also define the dimensionless quantities $K = 9ah^2/d^3$ and $D = k_B T/(Fb)$ to express the relative strengths of hydrodynamic and thermal forces, respectively. Then the equations of motion become

$$\frac{d\phi_1}{dt} = \omega_\phi - K\omega \cos(\phi_2 + \beta) \sin \phi_1 + \sqrt{2D\omega} \xi_1, \quad (3)$$

$$\frac{d\phi_2}{dt} = \omega_\phi - K\omega \cos(\phi_1 + \beta) \sin \phi_2 + \sqrt{2D\omega} \xi_2. \quad (4)$$

For typical flagella operating in water, we estimate the parameter values as $a \sim b \sim h \sim 1 \mu\text{m}$, $d \sim 10 \mu\text{m}$, $F \sim 10 \text{ pN}$, $k_B T \sim 4 \times 10^{-21} \text{ J}$ and $\eta \sim 10^{-3} \text{ Pa} \cdot \text{s}$. Thus

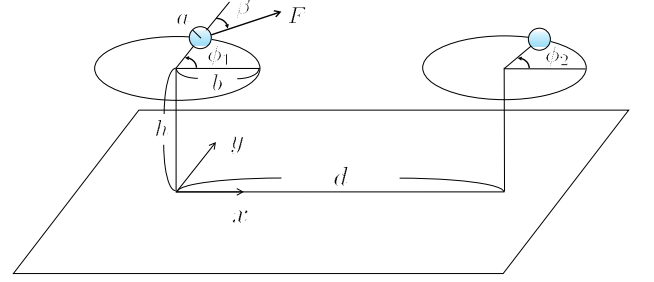


FIG. 1. (Color online) Schematic picture of the model of two flagella. Each sphere rotates on the circular trajectory of radius b , exerting the force F , which is tilted from the radial direction by the angle β in the clockwise direction, on the surrounding fluid.

we have $\omega \sim 10 \text{ Hz}$, $K \sim 10^{-2}$ and $D \sim 10^{-4}$. (Note that ω is not the flagellar rotation frequency, which is on the order of $10^2 - 10^3 \text{ Hz}$ and is not considered in the present model.)

III. STEADY STATE DISTRIBUTION

To analyze the system's behavior in the steady state, we first consider the case $\sin \beta \gg K, \sqrt{D}$, where the intrinsic phase velocity dominates the hydrodynamic and thermal ones (the second and third terms on the right-hand side of Eqs. (3),(4)), and introduce the slow variable $\Phi_i = \phi_i - \omega_\phi t$. Using these, we rewrite Eqs. (3), (4) as

$$\frac{d\Phi_1}{dt} = \frac{K\omega}{2} A(\Phi_2, \Phi_1) + \sqrt{2D\omega} \xi_1, \quad (5)$$

$$\frac{d\Phi_2}{dt} = \frac{K\omega}{2} A(\Phi_1, \Phi_2) + \sqrt{2D\omega} \xi_2, \quad (6)$$

where

$$A(\Phi_i, \Phi_j) = \sin(\Phi_i - \Phi_j + \beta) - \sin(\Phi_i + \Phi_j + 2\omega t + \beta). \quad (7)$$

The corresponding Fokker-Planck equation for the probability distribution function $P(\Phi_1, \Phi_2; t)$ read:

$$\frac{\partial P}{\partial t} = -\frac{K\omega}{2} \left\{ \frac{\partial}{\partial \Phi_1} [A(\Phi_2, \Phi_1)P] + \frac{\partial}{\partial \Phi_2} [A(\Phi_1, \Phi_2)P] \right\} + D\omega \left(\frac{\partial^2}{\partial \Phi_1^2} + \frac{\partial^2}{\partial \Phi_2^2} \right) P. \quad (8)$$

We integrate the equation over the period π/ω under the slow-variable approximation that Φ_i 's remain unchanged, to get the second term of $A(\Phi_i, \Phi_j)$ vanish. For the sta-

tionary state where $\partial P/\partial t = 0$, we obtain

$$0 = -\frac{K}{2} \left\{ \frac{\partial}{\partial \Phi_1} [\sin(\Phi_2 - \Phi_1 + \beta)P] + \frac{\partial}{\partial \Phi_2} [\sin(\Phi_1 - \Phi_2 + \beta)P] \right\} + D \left(\frac{\partial^2}{\partial \Phi_1^2} + \frac{\partial^2}{\partial \Phi_2^2} \right) P. \quad (9)$$

Solving the above equation, we obtain the steady-state distribution

$$P(\Phi_1, \Phi_2) = \frac{1}{Z} \exp \left[\frac{K}{2D} \cos \beta \cos(\Phi_2 - \Phi_1) \right], \quad (10)$$

or equivalently

$$P(\phi_1, \phi_2) = \frac{1}{Z} \exp \left[\frac{K}{2D} \cos \beta \cos(\phi_2 - \phi_1) \right], \quad (11)$$

in terms of the original variables, where Z is the normalization factor given by

$$Z = 16\pi^2 I_0 \left(\frac{K}{2D} \cos \beta \right). \quad (12)$$

Here, $I_0(x)$ is the 0-th order modified Bessel function. The steady state distribution (11) is the von-Mises distribution for the phase difference. The flagella are more likely to be synchronized ($\phi_1 = \phi_2$) for a stronger coupling K and weaker noise D . Synchronization is also facilitated by a smaller force angle β ; for $\beta = \frac{\pi}{2}$, the distribution becomes flat and the system shows no tendency toward synchronization. For a strong coupling, the harmonic approximation $\cos(\phi_2 - \phi_1) \sim 1 - \frac{1}{2}(\phi_2 - \phi_1)^2$ gives a Gaussian distribution of the phase difference $\delta = \phi_2 - \phi_1$ with the standard deviation $\sqrt{2D/(K \cos \beta)}$.

The stochastic entropy for a single state is defined by $s = -k_B \ln P$ [36]. Using the stationary distribution (11), we obtain

$$s(\phi_1, \phi_2) = k_B \left[\ln Z - \frac{K}{2D} \cos \beta \cos(\phi_2 - \phi_1) \right]. \quad (13)$$

The stochastic entropy is minimized when the two flagella are synchronized. This implies that the synchronized state is the most ordered state of the system, as stochastic entropy quantifies the degree of disorder.

IV. HEAT DISSIPATION

In stochastic thermodynamics, for a particle satisfying the overdamped Langevin equation

$$\gamma \dot{x} = F(x, t) + \sqrt{2\gamma T} \xi, \quad (14)$$

the heat dissipation during an infinitesimal displacement dx is defined as [36, 37]

$$dQ = F \circ dx = (\gamma \dot{x} - \sqrt{2\gamma T} \xi) \circ dx, \quad (15)$$

where \circ denotes the Stratonovich product. Applying the definition, the heat dissipation by the rotor 1 is written as

$$dQ_1 = \zeta b^2 [\omega_\phi - K\omega \cos(\phi_2 + \beta) \sin \phi_1] \circ d\phi_1. \quad (16)$$

For convenience, we normalize heat by ζb^2 and define

$$dQ'_1 = \frac{dQ_1}{\zeta b^2} = [\omega_\phi - K\omega \cos(\phi_2 + \beta) \sin \phi_1] \circ d\phi_1. \quad (17)$$

The heat dissipation by the rotor 2 is obtained similarly. The total heat dissipation in an arbitrary time period $0 < t < T$ under the initial condition $\phi_1(0) = \phi_2(0) = 0$ is obtained as, using partial integration,

$$\begin{aligned} Q' &= \int_0^T (dQ'_1 + dQ'_2) \\ &= \omega_\phi(\phi_1 + \phi_2) + K\omega [\cos(\phi_2 + \beta) \cos \phi_1 - \cos \beta] \\ &\quad + K\omega \int_0^{\phi_2} \sin \beta \cos(\phi_2 - \phi_1) \circ d\phi_2. \end{aligned} \quad (18)$$

Next we compute the heat specifically by solving the stochastic equations (3),(4) for the phase $\phi_i(t)$. We change the variables to $\delta = \phi_1 - \phi_2$ and $\sigma = \phi_1 + \phi_2$ in Eqs.(3),(4). For the phase difference, we obtain

$$\frac{d\delta}{dt} = -K\omega \cos \beta \sin \delta + 2\sqrt{D\omega} \xi_-, \quad (19)$$

where $\xi_- = (\xi_1 - \xi_2)/\sqrt{2}$. Assuming that the phase difference is small, we approximate $\sin \delta$ by δ and solve the equation as

$$\begin{aligned} \delta(t) &= 2\sqrt{D\omega} e^{-K\omega \cos \beta \cdot t} \int_0^t e^{K\omega \cos \beta \cdot s} dW_s \\ &= 2\sqrt{D\omega} \left(W_t - K\omega \cos \beta \int_0^t e^{K\omega \cos \beta \cdot (s-t)} W_s ds \right). \end{aligned} \quad (20)$$

Using this, we find $\langle \delta \rangle = \langle \phi_1 - \phi_2 \rangle = 0$ since the product is taken in Itô's sense. The variance reads

$$\begin{aligned} V(t) &= \langle \delta(t)^2 \rangle \\ &= 4D\omega e^{-2K\omega \cos \beta \cdot t} \int_0^t e^{2K\omega \cos \beta \cdot s} ds \\ &= \frac{2D}{K \cos \beta} - \frac{2D}{K \cos \beta} e^{-2K\omega \cos \beta \cdot t}. \end{aligned} \quad (21)$$

In the long time limit, it converges to the equilibrium value $2D/(K \cos \beta)$ from below. From this, we confirm that the small phase difference approximation is satisfied either when $2D/(K \cos \beta) \ll 1$ or in a sufficiently short time. The time-evolution equation of the phase sum σ is derived from Eqs.(3),(4) as

$$\frac{d\sigma}{dt} = 2\omega_\phi - K\omega \sin(\sigma + \beta) + K\omega_\phi \cos \delta + 2\sqrt{D\omega} \xi_+, \quad (22)$$

where $\xi_+ = (\xi_1 + \xi_2)/\sqrt{2}$. Using $\Phi_i = \phi_i - \omega_\phi t$ and $\Sigma = \Phi_1 + \Phi_2$ it can be rewritten as

$$\frac{d\Sigma}{dt} = K\omega \sin(\Sigma + \beta + 2\omega_\phi t) - K\omega \cos \delta \sin \beta + 2\sqrt{D\omega}\xi_+. \quad (23)$$

From this and Eq.(19), the change of Φ_i is proportional to the dimensionless parameters K and \sqrt{D} . that are in the slow variable approximation where $\sin \beta \gg K, \sqrt{D}$. We obtain Σ to the first order in K and \sqrt{D} as

$$\begin{aligned} \Sigma(t) = & K\omega_\phi t + \frac{K\omega}{2\omega_\phi} [\cos(2\omega_\phi t + \beta) - \cos \beta] \\ & + 2\sqrt{D\omega}W_t \end{aligned} \quad (24)$$

Retaining only the terms in the first order of K and \sqrt{D} in Eq.(20), we obtain $\delta(t) = 2\sqrt{D\omega}W_t$. Combining this and Eq.(24), and using the definition $\Phi_i = \phi_i - \omega_\phi t$, we obtain

$$\begin{aligned} \phi_i(t) = & \omega_\phi \left(1 + \frac{K}{2}\right) t + \frac{K\omega}{4\omega_\phi} [\cos(2\omega_\phi t + \beta) - \cos \beta] \\ & + \sqrt{2D\omega}W_t^{(i)} \end{aligned} \quad (25)$$

where W_i is Wiener process and the coefficient before that is also from the addition of two noise, and

$$\begin{aligned} Q'(t) = & 2\omega_\phi^2(1 + K)t - 2K\omega \sin(\omega_\phi t + \beta) \sin \omega_\phi t \\ & + 2\omega_\phi \sqrt{D\omega}W_t \end{aligned} \quad (26)$$

The first term shows the linear time dependence, the second term is periodic with the period π/ω_ϕ , and the last term is a Brownian term with increment of \sqrt{t} .

V. NUMERICAL ANALYSIS

In the analytical treatment, we used two approximations: (i) slow variable, and (ii) small phase difference. The approximation (i) holds for $\sin \beta \gg K, \sqrt{D}$, while (ii) is valid if $\cos \beta \gg D/K$. We used (i) to obtain the distribution (11), and (ii) for time-evolution of the phase difference (20), and both of them for in time-evolution of phase(25) and heat dissipation (26). In order to verify these results and study the cases beyond the approximations, we performed numerical analysis by varying β as the control parameter. We integrated Eqs.(3),(4) for the phases $\phi_i(t)$ using the Euler-Maruyama method, and Eq.(15) for Q'_1 and a similar equation for Q'_2 with $\phi(t + \Delta t/2) \simeq (\phi_i(t + \Delta t) + \phi_i(t))/2$ for the Stratonovich product using the semi-implicit scheme. The time increment $\Delta t = 10^{-4}$ is used for both sets of equations. We took 10^3 independent samples for the noise for statistical analysis. Below we focus on three representative cases: $\beta = 0.01\pi, 0.25\pi$, and 0.49π .

For $\beta = 0.01\pi$, the approximation (i) is not valid, while (ii) holds. Comparing the first and third terms

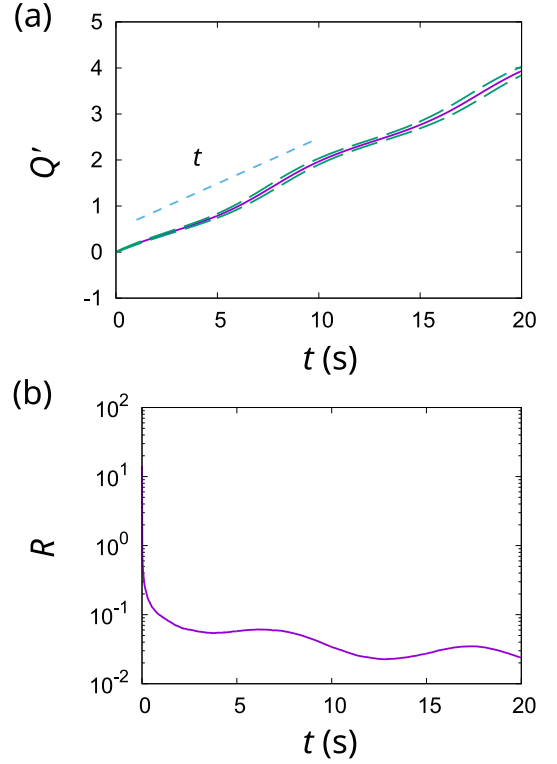


FIG. 2. (Color online) The case $\beta = 0.01\pi$. (a) Dimensionless heat versus time. The solid line shows the ensemble average $E_{Q'} = \langle Q' \rangle$ and the dashed lines show $E_{Q'} \pm \sigma_{Q'}$, where $\sigma_{Q'} = \sqrt{\langle Q'^2 \rangle - \langle Q' \rangle^2}$ is the standard deviation. The dotted line shows the slope $2\omega_\phi^2$. (b) The relative fluctuation $R = \sigma_{Q'}/E_{Q'}$ versus time (semi-log plot).

on the right hand side of Eq.(26), we expect a relatively large fluctuation effect for $t < \sqrt{D\omega}/\omega_\phi \sim 1$ s. We plot the mean $E_{Q'}(t) = \langle Q'(t) \rangle$ and the standard deviation $\sigma'_{Q'}(t) = \sqrt{\langle Q'(t)^2 \rangle - \langle Q'(t) \rangle^2}$ of the heat dissipation in Fig. 2(a) and the ratio $R = \sigma_{Q'}/E_{Q'}$ in Fig. 2(b). The ratio is large for short time, meeting our expectation. In Fig.2(a), $E_{Q'}(t)$ shows a feature of the superposition of linear increase and periodic motion. The slope of that is almost the same as $2\omega_\phi^2 \approx 0.2$ in (26). The curves also show a periodic part with period $T = 10$ s, which comes from the term $\sin(\omega_\phi t + \beta) \sin \omega_\phi t$.

For $\beta = 0.25\pi$, where both the approximations (i),(ii) are valid, we consider time-evolution of the variance of the phase difference $V_\delta(t) = \langle \delta^2 \rangle = \langle (\phi_2 - \phi_1)^2 \rangle$ and the variance of the heat dissipation $V_{Q'}(t) = \langle Q'(t)^2 \rangle - \langle Q'(t) \rangle^2$ in Fig.3. We choose the ending the time as 100s to see both initial and steady behavior. The results are in good agreement with our theoretical results; V_δ increases exponentially with time as in Eq.(20), while $V_{Q'}$ linearly increases with the slope $4\omega_\phi^2 D\omega = 0.2$ as in Eq.(26).

For $\beta = 0.49\pi$, the slow variable approximation holds but the small phase difference breaks down for a long time scale. We draw the temporal evolution of the variance of heat dissipation in Fig. 4. From the figure, we

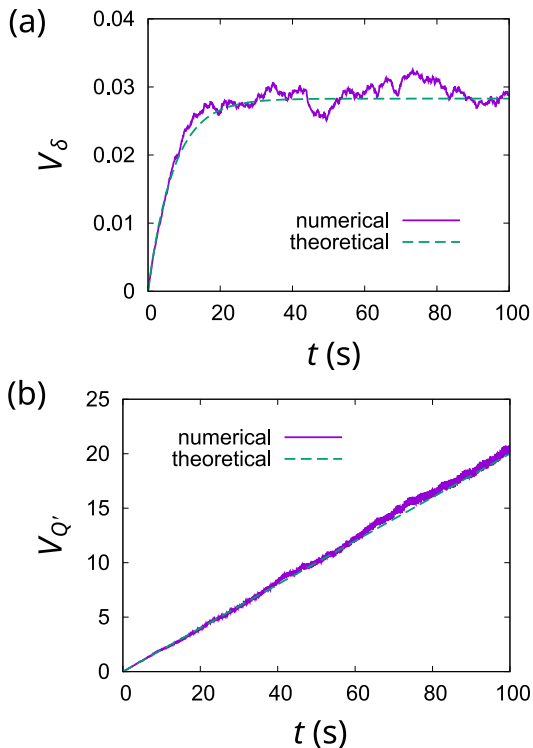


FIG. 3. (Color online) Variation of (a) the phase difference δ and (b) the dimensionless heat Q' versus time for $\beta = 0.25\pi$. The solid lines show the numerical results, and the dashed lines show the theoretical results [Eqs.(20),(26)]

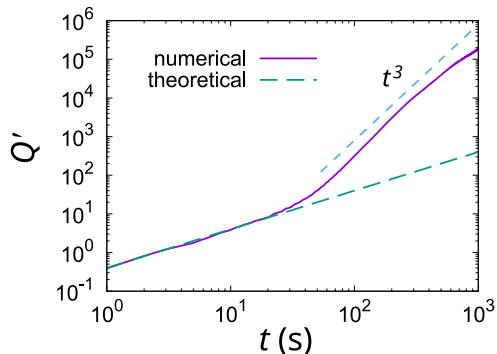


FIG. 4. (Color online) Variation of the dimensionless heat for $\beta = 0.49\pi$. The solid line shows the numerical result, the dashed line shows the theoretical result, and the dotted line shows the slope of t^3 .

find that in a small time, the variance increases linearly as shown by Eq.(26). However, in the long term, the variance approximately grows with a power law with the exponent 3, which is not predicted by the theory. The crossover behavior indicates that the fluctuation effects become more significant in the weakly synchronized state at the later stage.

Comparing the three cases, we find that the heat dissipation fluctuations at a given same time are larger for larger β . This is because the tendency toward synchronization (proportional to $\cos\beta$) decreases as β approaches $\pi/2$, making the effects of noise relatively large.

VI. DISCUSSION

In this paper, we proposed an analytical method to compute the motion and heat dissipation of interacting flagella for individual noise realizations. We solved the phase difference and heat dissipation explicitly under the the slow variable and strong coupling approximations. We compared the results with numerical simulations for three different parameter ranges, The results show a good correspondence where the two approximations are both valid. Our findings indicate that heat dissipation exhibits considerable dependence on noise realization and influences the energetics of bacterial flagellar synchronization. Experimentally, the bead trajectory obtained via a bead assay allows us to estimate the work done by the bead on the surrounding fluid as a function of time. Under the assumption of white noise, a short-time average of this work corresponds to the deterministic component, which is the heat dissipation (15). Thus, we anticipate that our results can be compared with experimental data to validate the features discussed above, which we leave for future work.

This study can be extended to analyze multiple flagella, enabling us to characterize heat dissipation in collective synchronization. For multi-flagellated bacteria such as *E. coli*, flagellar bundling is crucial for unidirectional propulsion. In such cases, active noise originating from flagellar motors such as fluctuations in the number of stators could play a significant role. Although our current model considers only thermal noise, it can be readily extended to include active noise, assuming that it is additive and temporally uncorrelated. Furthermore, because the model is of a generic form, it can be applied also to other mesoscale systems where thermodynamic noise affects but does not destroy synchronization.

Acknowledgment.— This work was supported by JSPS KAKENHI Grant Number JP24K06895 to N. U.

[1] A. Pikovsky, M. Rosenblum, and J. Kurths: *Synchronization: A Universal Concept in Nonlinear Sciences* (Cam-

bridge University Press, 2001).

[2] S. Strogatz: *Sync: The Emerging Science of Spontaneous*

- Order* (Penguin UK, 2004).
- [3] S. M. Reppert and D. R. Weaver: *Nature* **418** (2002) 935.
 - [4] O. Sporns: *Networks of the Brain* (MIT press, 2016).
 - [5] G. I. Taylor: *Proc. R. Soc. Lond. Ser. A* **209** (1951) 447.
 - [6] S. Gueron, K. Levit-Gurevich, N. Liron, and J. J. Blum: *Proc. Natl. Acad. Sci. U.S.A.* **94** (1997) 6001.
 - [7] S. Gueron and K. Levit-Gurevich: *Proc. Natl. Acad. Sci. U.S.A.* **96** (1999) 12240.
 - [8] R. Golestanian, J. M. Yeomans, and N. Uchida: *Soft Matter* **7** (2011) 3074.
 - [9] N. Uchida, R. Golestanian, and R. R. Bennett: *J. Phys. Soc. Jpn.* **86** (2017) 101007.
 - [10] N. Uchida and R. Golestanian: *Phys. Rev. Lett.* **106** (2011) 058104.
 - [11] J. Elgeti and G. Gompper: *Proc. Natl. Acad. Sci. U.S.A.* **110** (2013) 4470.
 - [12] D. R. Brumley, M. Polin, T. J. Pedley, and R. E. Goldstein: *J. Roy. Soc. Interface* **12** (2015) 20141358.
 - [13] F. Meng, R. R. Bennett, N. Uchida, and R. Golestanian: *Proc. Natl. Acad. Sci. U.S.A.* **118** (2021) e2102828118.
 - [14] B. M. Friedrich and F. Jülicher: *Phys. Rev. Lett.* **109** (2012) 138102.
 - [15] R. R. Bennett and R. Golestanian: *Phys. Rev. Lett.* **110** (2013) 148102.
 - [16] N. Naremsatsu, R. Quek, K.-H. Chiam, and Y. Iwadata: *Cytoskeleton* **72** (2015) 633.
 - [17] G. Quaranta, M.-E. Aubin-Tam, and D. Tam: *Phys. Rev. Lett.* **115** (2015) 238101.
 - [18] B. Chakrabarti, S. Fürthauer, and M. J. Shelley: *Proc. Natl. Acad. Sci. U.S.A.* **119** (2022) e2113539119.
 - [19] M. Reichert and H. Stark: *Eur. Phys. J. E* **17** (2005) 493.
 - [20] S. Y. Reigh, R. G. Winkler, and G. Gompper: *Soft Matter* **8** (2012) 4363.
 - [21] M. Tătulea-Codrean and E. Lauga: *Phys. Rev. Lett.* **128** (2022) 208101.
 - [22] J. Kotar, M. Leoni, B. Bassetti, M. C. Lagomarsino, and P. Cicutta: *Proc. Natl. Acad. Sci. U.S.A.* **107** (2010) 7669.
 - [23] R. E. Goldstein, M. Polin, and I. Tuval: *Phys. Rev. Lett.* **103** (2009) 168103.
 - [24] Y.-T. Hsiao, K.-T. Wu, N. Uchida, and W.-Y. Woon: *Appl. Phys. Lett.* **108** (2016).
 - [25] H. Sakaguchi: *Prog. Theor. Phys.* **79** (1988) 39.
 - [26] J.-n. Teramae and D. Tanaka: *Phys. Rev. Lett.* **93** (2004) 204103.
 - [27] Y. Izumida, H. Kori, and U. Seifert: *Phys. Rev. E* **94** (2016) 052221.
 - [28] H. Hong, J. Jo, C. Hyeon, and H. Park: *J. Stat. Mech.* **2020** (2020) 074001.
 - [29] X. Yang, M. Heinemann, J. Howard, G. Huber, S. Iyer-Biswas, G. Le Treut, M. Lynch, K. L. Montooth, D. J. Needleman, S. Pigolotti, et al.: *Proc. Natl. Acad. Sci. U.S.A.* **118** (2021) e2026786118.
 - [30] M. Silverman and M. Simon: *Nature* **249** (1974) 73.
 - [31] W. S. Ryu, R. M. Berry, and H. C. Berg: *Nature* **403** (2000) 444.
 - [32] Y. Sowa, A. D. Rowe, M. C. Leake, T. Yakushi, M. Homma, A. Ishijima, and R. M. Berry: *Nature* **437** (2005) 916.
 - [33] S. Nakamura, Y. Hanaizumi, Y. V. Morimoto, Y. Inoue, M. Erhardt, T. Minamino, and K. Namba: *Mol. Microbiol.* **113** (2020) 755.
 - [34] N. Uchida and R. Golestanian: *Phys. Rev. Lett.* **104** (2010) 178103.
 - [35] J. R. Blake: *Math. Proc. Camb. Philos. Soc.* **70** (1971) 303.
 - [36] N. Shiraishi: *An Introduction to Stochastic Thermodynamics* (Springer, 2023).
 - [37] K. Sekimoto: *Stochastic Energetics* (Lecture Notes in Physics. Springer Berlin Heidelberg, 2010), Lecture Notes in Physics.